Korean J. Chem. Eng., 37(12), 2202-2208 (2020)
DOI: 10.1007/s11814-020-0637-8

pISSN: 0256-1115
eISSN: 1975-7220

High capacity ethidium bromide removal by montmorillonites

Lijuan Wang*, Zhaohui Li*,,†, Xingrong Zhang***, Guocheng Lv*, and Xisen Wang******

*Beijing Key Laboratory of Materials Utilization of Nonmetallic Minerals and Solid Wastes,
National Laboratory of Mineral Materials, School of Materials Science and Technology,
China University of Geosciences, Beijing, 29 Xueyuan Road, Beijing, China 100083
**Department of Geosciences, University of Wisconsin - Parkside, 900 Wood Road, Kenosha, WI 53144, USA
***BGRIMM Technology Group, Beijing 110160, China
****Department of Chemistry, University of Wisconsin - Parkside, 900 Wood Road, Kenosha, WI 53144, USA

(*Received 1 May 2020 • Revised 7 July 2020 • Accepted 11 July 2020*)

Abstract−Ethidium bromide (EtBr) is commonly used as a reagent to investigate DNA and RNA bonding in biochemistry. However, it is mutagenic and toxic; thus, its removal from the waste solution is of the top priority in lab safety practice. Although many products with high EtBr removal capacities are available on the market, developing new products with low material costs and high removal capacities is still an urgent priority. As the EtBr is in a cationic form Et^+ balanced by counterion Br^- in aqueous solution, materials with high cation exchange capacity and large specific surface area may have great potential for efficient EtBr removal, Thus, several montmorillonites (MMTs) were evaluated for their EtBr removal capacity and methods of regeneration in this study. Results showed that both external and internal surfaces of MMTs were effective sorption sites for EtBr with a capacity up to 600 mg/g. And the waste-laden materials could be regenerated or safely disposed after incineration at 500 °C for 2 h. As such, further tests on optimization and manufacturing kits or devices for practical EtBr removal in routine lab practice is of engineering priority, should MMTs be further explored as an effective material for EtBr removal.

Keywords: Destruction, Ethidium Bromide, Montmorillonite, Removal, Regeneration

INTRODUCTION

Ethidium bromide (3,8 diamino-5-ethyl-6-phenyl phenanthridinium bromide) (EtBr) is a dark red, crystalline material. Because of its fluorescence when bound to double stranded-DNA and single-stranded RNA, it is commonly used in gel electrophoresis applications for visualization of these molecules. However, EtBr is mutagenic and moderately toxic, so proper disposal of the waste is required.

Six different methods for the destruction of EtBr in solutions were compared, with the best method being treatment with hypophosphorous acid and sodium nitrite, which can convert EtBr to non-mutagenic degradation products by 99.8% [1]. For sorptive removal, different sorbents were evaluated including Amberlite XAD-16 [1], activated charcoal filter [2], and carbon nanotubes [3]. However, the EtBr removal capacity was relatively low for these materials. The Langmuir sorption capacity of EtBr on the carbon nanotubes was only 0.8 mg/g [3]. Similarly, the uptake of EtBr on graphene oxides was only 0.45 mg/g [4].

Commercially available products for sorptive removal of EtBr from solution include EtBr Green Bag Disposal Kit manufactured by Thomas Scientific [5] and MP Biomedicals [6]. Each bag has a capacity of 10 mg EtBr removal. The packing materials were not disclosed but activated materials were stated.

Earth materials refer to naturally occurring materials, including rocks, minerals, and soils. They are low in material cost and vast in resource reserves. As such, interactions between earth materials and anthropogenic compounds have attracted great attention since the 1990's. Commonly used earth materials for the removal of environmental contaminants include, but are not limited to, clay minerals and zeolites, due to their low material cost and high specific surface area (SSA) and cation exchange capacity (CEC). However, most of the research on using Earth materials for contaminant removal is focused on heavy metals, such as Hg(II), Pb(II), and Zn(II) [7], Pb(II), Cu(II), and Cd(II) [8] and color dyes [9]. Tested earth materials for the removal of EtBr are limited. They include kaolinite at a capacity of 0.15 mmol/g [10], modified diatomite at 0.3 mmol/g [11], modified sepiolite at 4.3 mg/g [12], pumice at 77 mg/g [13], and rectorite at 0.4 mmol/g or 160 mg/g [14].

Montmorillonite (MMT) is a type of phyllosilicate that has high CEC and SSA values. In a previous study, cation exchange was believed to be the dominant mechanism for EtBr removal by rectorite [14], a type of phyllosilicate with a CEC of 400 $mmol_c$/kg in comparison to 1,200 $mmol_c$/kg for some MMTs. However, EtBr removal by MMTs has not been reported. Thus, the novelty of the current study was to explore the use of MMTs for the removal of EtBr from solution, so that minimal waste disposal would be needed after EtBr removal, or heat regeneration of spent MMT could be achieved. The specific objectives were to evaluate EtBr removal capacity and kinetics using MMT in comparison to currently commercially available materials, and to decipher the mechanisms of EtBr removal using modern instruments in conjunction with molecular dynamic simulations.

---

†To whom correspondence should be addressed.
E-mail: li@uwp.edu

MATERIALS AND METHODS

1. Materials

The EtBr (Fig. S1) used has a CAS # of 1239-45-8, a formula of $C_{21}H_{20}BrN_3$, a molar mass of 394.294 g/mol, and a water solubility of 40 g/L. It is in a cationic form with Br^- as the counterion in aqueous solution; the two amino groups at positions 7 and 2 could be further protonated at pH 2.43 (pK_{a2}) and 0.71 (pK_{a1}) [15]. It may form dimers with a reported equilibrium constant of $30\pm10\ M^{-1}$ [16], which results in monomer and dimer concentrations of 7 and 3 mM with an initial EtBr concentration of 10 mM.

The earth materials used were phyllosilicates MMTs and tectosilicate zeolite because of their high CEC values. The MMTs were obtained from the Clay Minerals repository. They are SWy-2, from Wyoming, with Na^+ as the interlayer cation with one layer of water; SAz-2, from Arizona, and STx-1b, from Texas, both have Ca^{2+} as the interlayer cation with two layers of water. The zeolite was a clinoptilolite provided by the St. Cloud mine in Winston, NM. Their physico-chemical properties are listed in Table 1. Also tested were graphite, powder activated carbon (PAC), and packing material for filters in a commercial EtBr removal device, so that the results of this study can be compared with those of commercial available materials.

2. Experiments

For the isotherm study, 1.00 g of the MMTs and 100 mL of EtBr solutions at concentrations of 0 to 20 mmol/L were placed to each 200 mL centrifuge bottles and mixed for 24 h at 150 rpm. The purpose of using large quantities of MMTs was to evaluate the heat destruction and regeneration of the spent MMTs and use of the regenerated MMTs for further EtBr removal. For zeolite, graphite, PAC, and filter materials, 0.1 of solid and 10 mL of EtBr solutions were used, only to compare the results to the EtBr removal by MMTs. After being centrifuged, the supernatants were filtered through 0.45 μm syringe filters and analyzed for the equilibrium EtBr concentration by a UV-Vis spectrophotometric method. The solids were dried in aluminum weighing boats under room temperature. Then, a fraction of them was instrumentally characterized, while the majority was heat-regenerated and EtBr removal retested. These experiments served as the foundation for EtBr sorption isotherm study to evaluate EtBr removal capacity by these materials.

For the kinetic study, 1.00 g of the MMTs and 100 mL of EtBr solutions at an initial concentration of 10 mmol/L were placed to each 200 mL centrifuge bottles and mixed for 0.1, 0.25, 0.5, 1.0, 2.0, 4.0, 8.0, and 24.0 h at 150 rpm. At each time, 2-3 mL of the solution was removed from the bottles and filtered through 0.45 μm syringe filters and then analyzed by UV-Vis after proper dilution.

For the tea bag experiment, 1.0 g of MMT was placed in a nylon tea bag and sealed. The bag was dipped into EtBr solutions at an initial concentration of 1.0 mM for about 10 min with swirling. Then EtBr concentration in solution was analyzed by UV-Vis. The goal of this experiment was to explore future fabrication of MMT for convenient removal of EtBr from spent solutions in biochemistry.

Regeneration was made by heating the EtBr-laden solids at 500 °C for 2 h. Then, 0.1 g of the regenerated sample was mixed with 10 mL of EtBr solutions at 2.67 and 5.00 mmol/L for 24 h to evaluate the efficiency of heat regeneration. For all experiments, duplicates were conducted for each experimental condition.

3. Instrumental Analyses

Equilibrium EtBr concentrations were determined using a UV-Vis spectrophotometer (SmartSpec 3000, Bio-Rad Corp.) at the wavelength of 480 nm [17]. Powder X-ray diffraction (XRD) analyses were performed on an XRD-6100 diffractometer (Shimadzu) with Ni-filtered CuKα radiation operated at 30 kV and 40 mA. Oriented samples were scanned in the 2θ range of 2-32°. A 0.3 mm receiving slit and 1° divergent slit were used. The Fourier transform infrared (FTIR) spectra were acquired on a Shimadzu 8100 spectrometer equipped with a diamond attenuated total reflection

Table 1. Physico-chemical properties of materials for EtBr removal and their prices

Samples	EtBr removal capacity (mmol/kg)	CEC ($mmol_c$/kg)	N_2 SSA (m^2/g)	Price ($/ton)	FoM (mol/$)
SAz-2 [23]	1,500	1,200	97	77 as of 2018 [24]	14,576
SWy-2 [23]	1,200	760	32	77 as of 2018 [24]	11,818
STx-1b [23]	1,100	840	84	77 as of 2018 [24]	6,277
Zeolite [18]	120	110 for ECEC 800 for total CEC	16	140 [24]	<857
PAC	1,200			660-1,600 &	660-1,600
Filter materials	800				
Graphite	Linear isotherm			420-1,840 [24]	574-2,515
Rectorite [14]	400	410	10		
Kaolinite [10]	150			140 [24]	<1,070
Modified Sepiolite [12]	11			380-600# for unmodified	<18-29
Modified diatomite [11]	300			380 [24] for unmodified	<789
Pumice [13]	190			30 [24]	<6,333

& https://www.alibaba.com/showroom/powdered-activated-carbon-price.html

https://www.alibaba.com/showroom/sepiolite-fiber-price.html

For those with < sign, the FoM values were calculated based on the EtBr sorption capacity, as the 10% of the maximal input concentration was not available.

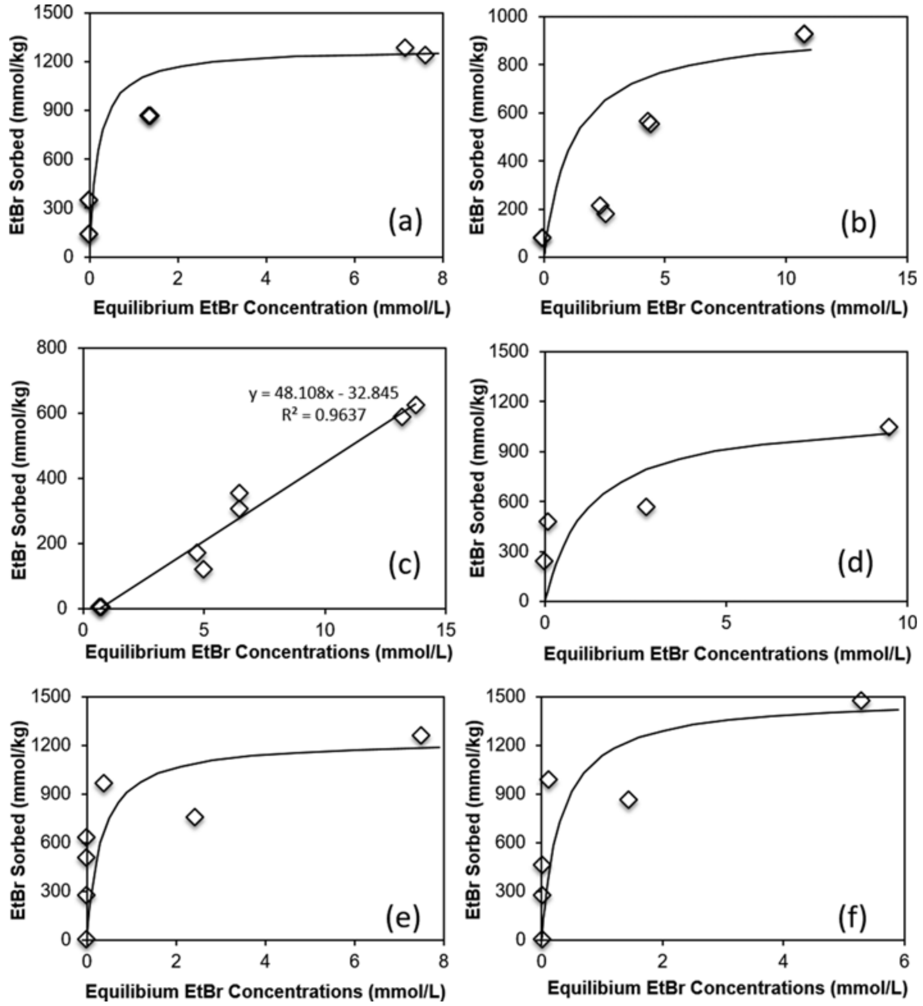

Fig. 1. EtBr sorption isotherms on PAC (a), Filter (b), Graphite (c), STx-1 (d), SWy-2 (e), and SAz-2 (f). The lines are the Langmuir fits to the observed data.

device. Samples were scanned from 400 to 4,000 cm^{-1} with a nominal resolution of 4 cm^{-1}. A scanning electron microscope (SEM) (Gemini 300, ZEISS, Germany) was used for morphological observation. The energy dispersion spectrum (EDS) was obtained using XFlash® 5010 silicon drift detector (Bruker) attached to the SEM. Thermogravimetric (TG) analyses were performed on a Shimadzu TGA-50 with a heating rate of 10 °C/min under air condition. The initial sample weight was between 5 and 7 mg.

4. Molecular Dynamic Simulation

A molecular dynamic simulation was conducted using 'FORCITE' module in Materials Studio 6.0 software to investigate the interlayer configuration of intercalated EtBr molecules. The supercells were built based on 4ax4b of the unit cell of MMT. The number of EtBr molecules used was based on the total surface area of 760 m^2/g and the EtBr sorption capacity on SAz-2 at 1,500 mmol/kg. The constructed model was optimized geometrically with a temperature at 298 K.

RESULTS AND DISCUSSION

The removal of EtBr by five of the six selected materials followed the Langmuir sorption isotherm (Fig. 1), suggesting a capacity limited removal, perhaps due to SSA or CEC constraint. The EtBr removal capacities were 1,200, 800, 1,100, 1,200, and 1,500 mmol/kg for PAC, filter materials, STx-1b, SWy-2, and SAz-2, respectively. These results indicated that the MMTs are comparable or even better than the commercial materials currently available on the market. However, the material costs of MMTs are just a fraction of those commercially available materials for EtBr removal (Table 1).

Their EtBr removal capacity was much higher than 400 mmol/kg for rectorite, which is a mixed layered clay mineral made of 1 : 1 layer of illite : MMT [14], and other earth materials and modified earth materials [10-13] (Table 1). In contrast, the uptake of EtBr on graphite followed a linear isotherm, suggesting a partitioning mechanism for EtBr removal by graphite. For the zeolite, the EtBr capacity was only 120 mmol/kg (Data not presented), much lower than its total CEC value of 800 mmol_c/kg, but close to its external CEC value of 110 mmol_c/kg [18], as the EtBr molecules are too large to enter into the internal cation exchange sites. As such, zeolite was no longer considered for further investigation.

The figure of merit (FoM), a criterion to assess the overall effi-

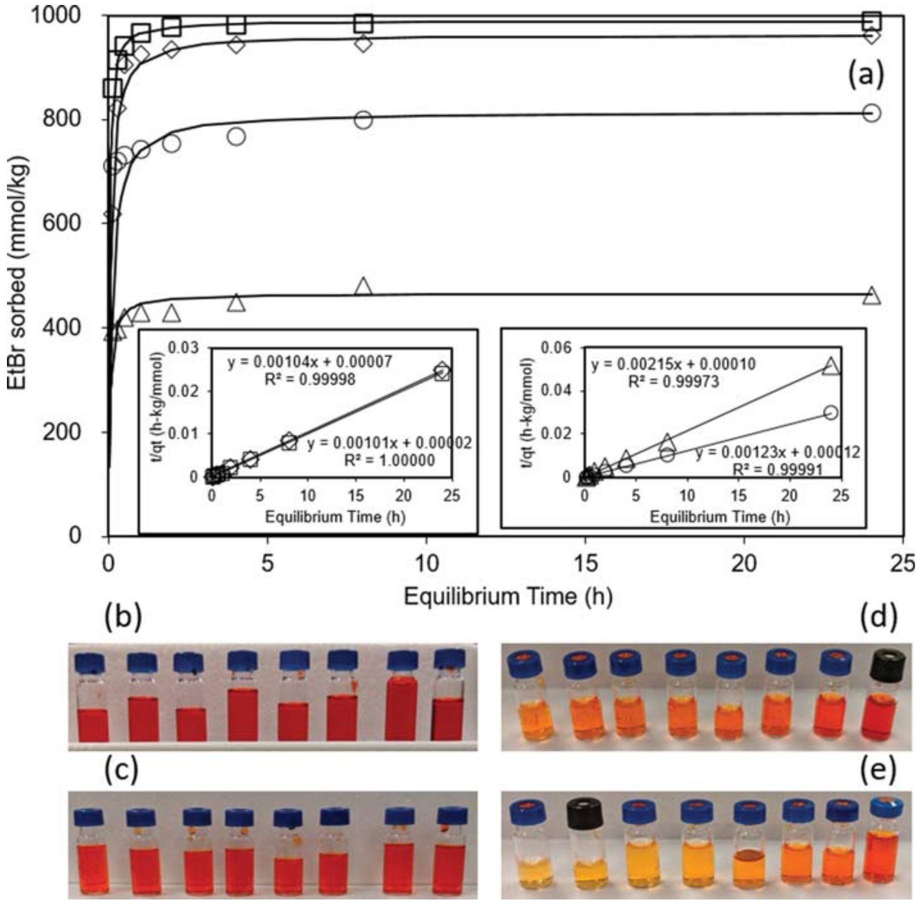

Fig. 2. Kinetics of EtBr sorption (a) on Filter (circle), PAC (triangle), SWy-2 (diamond), and SAz-2 (square). The lines are the pseudo-second order to the observed data. The insets are the fits to the linearized pseudo-second order equation. And progressive decrease in supernatant EtBr concentrations after equilibrated with 0.1, 0.25, 0.5, 1.0, 2.0, 4.0, 8.0, and 24.0 h (from right to left of each picture) by Filter (b), PAC (c), SWy-2 (d), and SAz-2 (e).

ciency of the sorbent, for sorptive removal of contaminants, was described by 10% breakthrough volume (BTV_{10}, L/g) divided by sorbent cost (USD/kg) for column studies [19]. However, with different initial concentrations, the BTV_{10} would be different for the same sorbent. For batch study, the BTV_{10} was not available. However, if the amount sorbed (mmol/kg) at 10% of the input concentration divided by the sorbent cost ($/kg) was used as the FoM for batch studies, it might also give some cost and efficiency comparison for each sorbent. The FoM values were much high for MMTs in comparison to other sorbents (Table 1), suggesting favorable potential use for the removal of EtBr from solution.

Kinetically, EtBr removal by MMTs is relatively fast (Fig. 2). The data fitted to the pseudo-second order reaction well with initial rates of 40,000 and 15,000 mmol/kg-h and sorption maxima of 989 and 963 mmol/kg for SAz-2 and SWy-2, respectively. In contrast, the initial rates were 8,000 and 10,000 mmol/kg-h and sorption maxima were 815 and 466 mmol/kg for PAC and filter material. The equilibrium Br^- concentrations were about 20-30% lower than the input concentration and were invariable with time as revealed by HPLC analyses (data not shown), confirming that most of the sorbed EtBr was in cationic form of Et^+ with some bilayer formations with Br^- as the counterion because of direct dimer sorption. More drastic change in color with time was noticed for MMTs in comparison to PAC and filter material (Fig. 2(b)-(e)).

Instrumental characterization was limited to SWy-2 and SAz-2. The oriented XRD analyses showed their characteristic peaks of (001) and (003), confirming their interlayer cations of Na^+ and Ca^{2+} with one or two layers of water (Fig. 3). At the EtBr loading of 760 and 860 mmol/kg, their d_{001} spacing expanded accordingly to 1.67 and 1.81 nm, respectively, confirming the interlayer uptake of EtBr from solution.

After being heated at 500 °C for 2 h, the XRD patterns showed reduction of d_{001} spacing, suggesting destruction of the intercalated EtBr. EtBr uptake from a dilute solution resulted in loading of 100 and 180 mmol/kg on regenerated SWy-2 and SAz-2, respectively. Due to the lower loading levels, the d_{001} spacing did not expand much, suggesting that the uptake of EtBr on heat regenerated MMT may be limited to the external surfaces (Fig. 3).

The TG analysis of raw SAz-2 showed a weight loss of about 20% at 550 °C (Fig. 4). In contrast, the crystalline EtBr showed a weight loss of about 55% at 550 °C. The weight loss of EtBr-loaded SAz-2 at a loading level of 1,500 mmol/kg reached about 60%. The much larger weight loss was attributed to decomposition of sorbed/intercalated EtBr. The DTG curve of raw SAz-2 showed two tem-

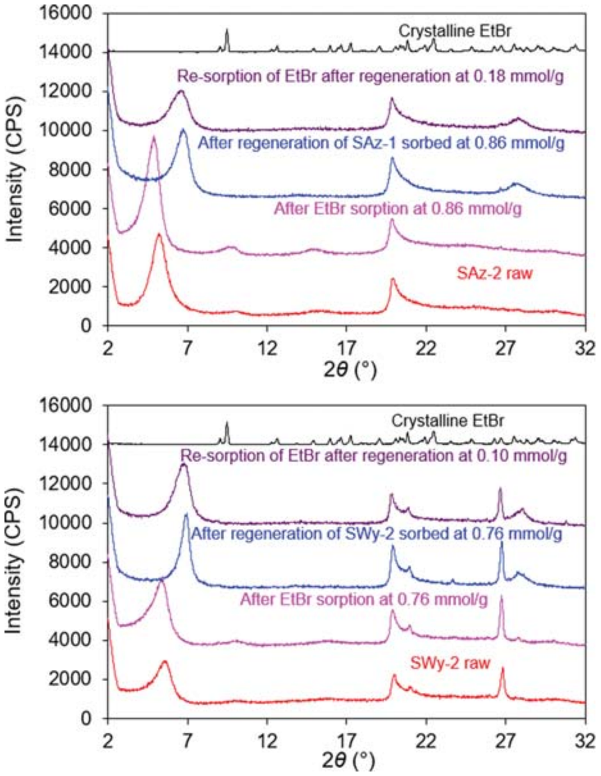

Fig. 3. XRD patterns of MMT loaded with EtBr before and after regeneration at 500 °C. Top: SAz-2. Bottom: SWy-2.

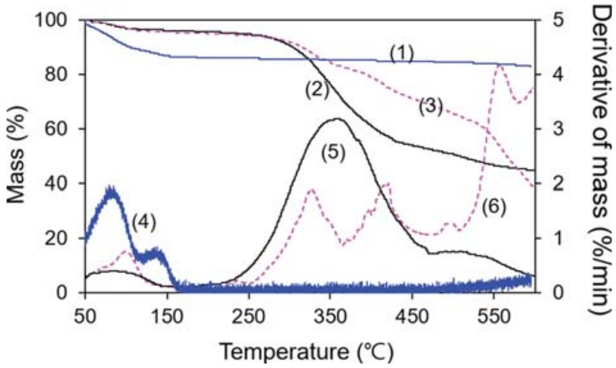

Fig. 4. TG analyses (left Y-axis) of SAz-2 (1), EtBr (2), and EtBr loaded SAz-2 (3) and their DTG analysis (right Y-axis) (4)-(6).

peratures at 70 and 125 °C, corresponding to the removal of surface sorbed water and interlayer water, respectively [20]. For crystalline EtBr, the peak decomposition temperature (T_{peak}) occurred at 340 °C, in comparison to 220 °C in a previous study [2]. For the EtBr loaded SAz-2, the DTG curve showed peaks at 107, 317, 405, and 557 °C (Fig. 4), corresponding to the removal of sorbed water, decomposition of EtBr sorbed on the external surfaces and in the interlayer [14], and perhaps, the final mineralization to form CO_2. The DTG results not only confirmed that the EtBr molecules replaced the hydrated Ca^{2+} ions in the interlayers [21], but also supported that the decomposition of EtBr from the internal surface of SAz-2 occurred in addition to the external surface of the clay mineral [22]. The last peak may suggest that the regeneration at 500 °C may not completely clean the interlayer space for resorption of EtBr.

The SEM observation showed no changes in crystal morphology after heat regeneration (Fig. S2), suggesting that the temperature was not high enough to destroy the crystal structure, as indicated

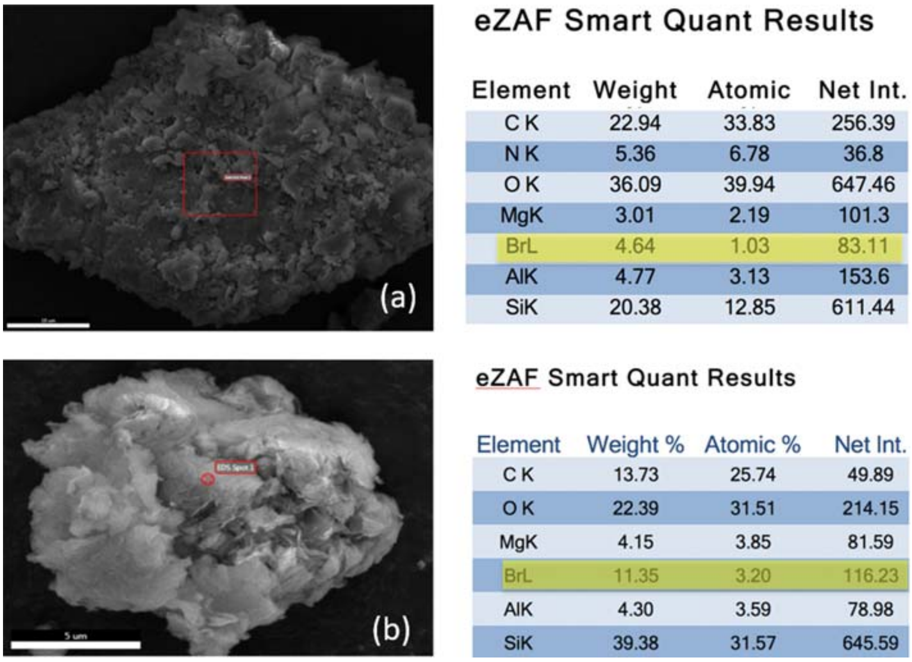

eZAF Smart Quant Results

Element	Weight	Atomic	Net Int.
C K	22.94	33.83	256.39
N K	5.36	6.78	36.8
O K	36.09	39.94	647.46
MgK	3.01	2.19	101.3
BrL	4.64	1.03	83.11
AlK	4.77	3.13	153.6
SiK	20.38	12.85	611.44

eZAF Smart Quant Results

Element	Weight %	Atomic %	Net Int.
C K	13.73	25.74	49.89
O K	22.39	31.51	214.15
MgK	4.15	3.85	81.59
BrL	11.35	3.20	116.23
AlK	4.30	3.59	78.98
SiK	39.38	31.57	645.59

Fig. 5. SEM pictures and EDS results of regenerated SAz-2 (a) and regenerated SAz-2 after re-equilibrated with 10 mM EtBr solution (b). The SAz-2 was initially equilibrated with EtBr solution at a concentration of 10 mM for 24 h. After which the spent SAz-2 was heated to 500 °C for 2 h to break down EtBr and to regenerate SAz-2. The Br level indicated the presence of Br on the surface or in the interlayer of SAz-2 after EtBr breakdown. The increase in Br level confirmed the efficiency of regeneration.

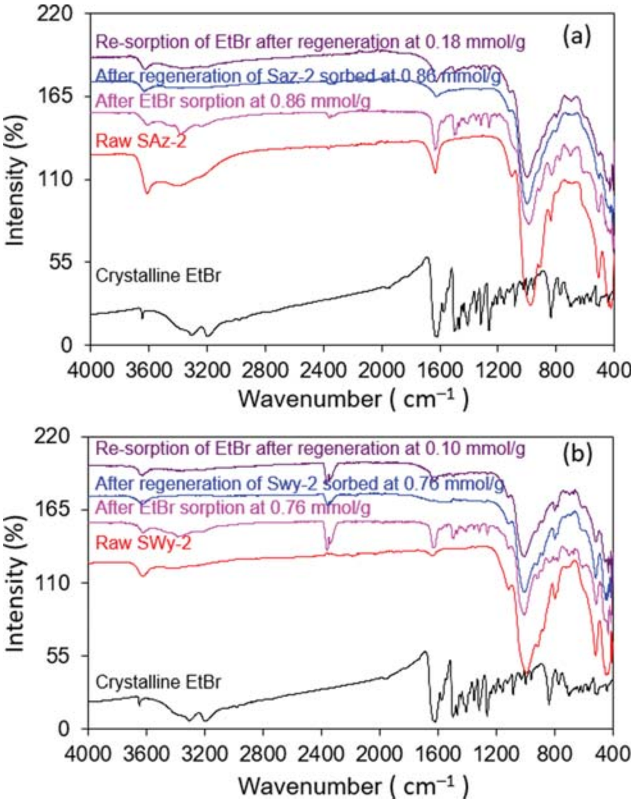

Fig. 6. FTIR spectra of SAz-2 (a) and SWy-2 (b) loaded with EtBr before and after regeneration at 500 °C.

Table 2. FTIR bands for EtBr and EtBr sorbed on MMT

EtBr [25]	Crystalline EtBr this study	EtBr on MMT	Possible assignments
3,302 vs	3,296	3,371	ν(N-H)
1,629 vs	1,618	1,626	δ(N-H)
1,499 vs	1,495	1,497	ν(C=N)
1,489 vs	1,464	1,464	ν(C=C) (in-ring), aromatic
1,408 s	1,404	1,404	ν(C-H)
1,352 ms	1,350	1,346	ν_{as}(C-N)
1,319 vs	1,315	1,314	ν_s(C-N)
1,262 vs	1,263	1,257	δ(C-H) in plane bending

by the XRD results. Meanwhile, the EDS data showed the presence of Br after heat regeneration of spent SAz-2 and increased Br contents after re-sorption of EtBr using regenerated SAz-2 (Fig. 5).

The FTIR results (Fig. 6) also confirmed the uptake and retention of EtBr on both minerals. The band assignments are listed in Table 2. The most important change was the significant increase in wavenumbers of 3,296 and 1,618 cm^{-1}, corresponding to ν(N-H) and δ(N-H), after EtBr sorption on MMT (Fig. 6 and Table 2), strongly suggesting involvement of N$^+$ in the bonding with MMT. The bands corresponding to EtBr were absent for heat-treated samples, indicating the decomposition of EtBr after being heated at 500 °C for 2 h. In comparison to raw MMT, the heat-treated samples lost the interlayer water (lack of a broad band at 3,400 cm^{-1}), confirming the dehydration as observed by XRD analyses.

Using the total SSA of 760 m^2/g and the EtBr sorption capacity of 1,500 mmol/kg, the calculated surface area occupied per EtBr molecule would be about 85 Å^2. On the other hand, the flat lying EtBr is at least 110 Å^2 (Fig. S1). Even the total SSA is thus not enough for a monolayer EtBr sorption in the interlayer of MMT. Therefore, either tilted or a patch bilayer EtBr formation is needed to intercalate into the interlayer of MMT. Molecular dynamic simulation showed that the intercalated EtBr took a bilayer configuration in the interlayer space of MMT with a close interaction between the amine and the negatively charged mineral surfaces (Fig. 7), confirming the FTIR results. With an initial EtBr concentration of 10 mM, the dimer concentration would be between 3 and 5.5 mM [14]. Thus, both the XRD results and molecular simulation confirmed the bilayer EtBr formation in the interlayer of MMT, which accounts for the high EtBr removal capacity.

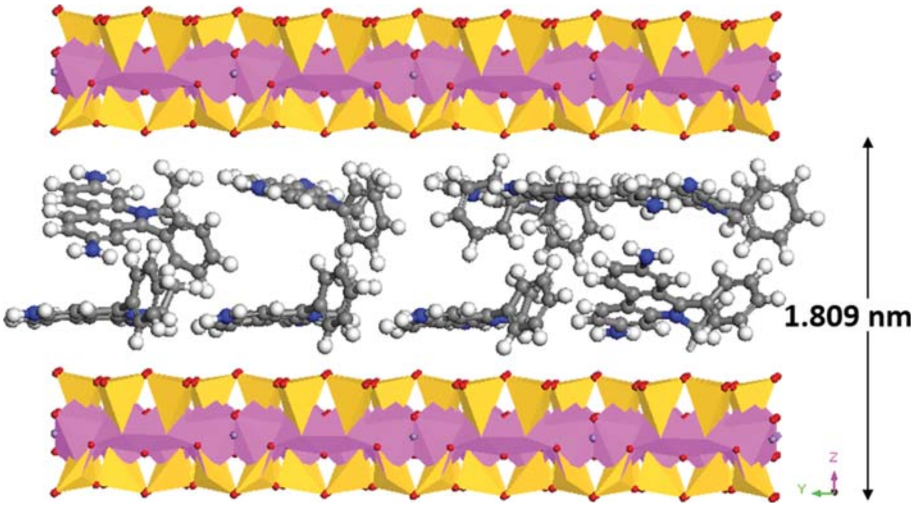

Fig. 7. Molecular dynamic simulation showing intercalation of EtBr aggregates in the form of bilayer in the interlayer of SAz-2 at the loading level of 1,500 mmol/kg.

The results of the above studies show that the EtBr sorption capacity was slightly larger than the CEC of the MMTs, the uptake of counterion Br^- was limited, the location of the sorption was both on the external and internal sites of MMTs, and the involvement of the interactions between protonated N^+ in EtBr with negatively charged MMT surfaces, and the uptake of EtBr was SSA and CEC limited. Thus, this study further confirms a previous mechanistic study on the uptake of EtBr on rectorite [14].

Ethidium bromide staining solution is of a final concentration of approximately 0.2-0.5 μg/mL (usually about 2-3 μL of lab stock solution per 100 mL gel). As such, 1 μM is about 0.4 mg/L. However, our analytical methods had a detection limit of 10 μm. Thus, in the tea bag experiment, a tea bag of 1 g of SAz-2 was dipped into 100 mL of 1 mM solution (39 mg) for 10 min. The final concentration dropped to 0.07 mM, about 93% EtBr removal, or 35 mg of EtBr removal. However, the final concentration was still above (70 times) the working concentration of EtBr in gel staining solution. As the preliminary tests were intended to explore the EtBr removal capacity, further treatment of the water with low initial concentration is needed with a sensitive EtBr detection.

As EtBr can be destroyed by heating at temperature above 262 °C, incineration of the contaminated charcoal filters would be a simple and cheap decontamination procedure [2]. In this study, after heat regeneration, the sorbents would be reused instead of being disposed, adding another advantage of using MMT for EtBr removal.

CONCLUSIONS

Selected earth materials with high CEC and SSA values were tested for their removal of EtBr from solution and compared to commercial available materials in terms of EtBr removal capacity, kinetics, and MoF. Modern instrument analyses in conjunction with molecular dynamic simulation were conducted to decipher the mechanism of EtBr removal. Through this study it was found that the MMT was inexpensive in materials cost, effective in EtBr removal, could be regenerated and heat-destructed for the spent material. Moreover, due to the swelling feature, the interlayer space MMT is available for uptake of EtBr. Due to the extremely high EtBr removal capacity, minimal amounts of spend sorbents would need to be decomposed. The high EtBr removal capacity was attributed to the large specific surface area and high cation exchange capacity of MMT. Thus, MMT is an extremely prospective earth material for the manufacture of testing kits or devices for EtBr removal from solution.

ACKNOWLEDGEMENTS

The research was supported by a Prototype Development Fund from Wisys Technology Foundation, Inc. and by Beijing Natural Science Foundation (2192048).

SUPPORTING INFORMATION

Additional information as noted in the text. This information is available via the Internet at http://www.springer.com/chemistry/journal/11814.

REFERENCES

1. G. Lunn and E. B. Sansone, *Anal. Biochem.*, **162**, 453 (1987).
2. F. D. Menozzi, A. Michel, H. Pora and A. O. A. Miller, *Chromatographia*, **29**, 167 (1990).
3. O. Moradi, M. Norouzi, A. Fakhri and K. Naddafi, *J. Environ. Health Sci. Eng.*, **12**, 17 (2014).
4. M. Rajabi, O. Moradi and K. Zare, *Int. Nano Lett.*, **7**, 35 (2017).
5. https://www.thomassci.com/Equipment/Electrophoresis-Systems/_/EtBr-Green-Bag-Disposal-Kit.
6. https://www.mpbio.com/etbr-greenbag-disposal-kit-50-bag.
7. R. Celis, M. C. Hermosin and J. Cornejo, *Environ. Sci. Technol.*, **34**, 4593 (2000).
8. L. Y. Li, *Environ. Technol.*, **27**, 811 (2006).
9. A. A. Adeyemo, I. O. Adeoye and O. S. Bello, *Appl. Water Sci.*, **7**, 543 (2017).
10. R. G. Harris, J. D. Wells and B. B. Johnson, *Colloids Surf. A*, **180**, 131 (2001).
11. H. Yu and B. Fugetsu, *J. Hazard. Mater.*, **177**, 138 (2010).
12. C. Cheng, L. Ma, J. Ren, L. Li, G. Zhang, Q. Yang and C. Zhao, *Chem. Eng. J.*, **171**, 1132 (2011).
13. B. Heibati, K. Yetilmezsoy, M. A. Zazouli, S. Rodriguez-Couto, I. Tyagi, S. Agarwal and V. K. Gupta, *J. Mol. Liq.*, **213**, 41 (2016).
14. Z. Li, P. H. Chang, W. T. Jiang and Y. Liu, *J. Hazard. Mater.*, **384**, 121254 (2020).
15. Z. Zimmermann and H. W. Zimmermann, *Zeitschrift für Naturforschung C*, 31656 (1976).
16. G. Thomas and B. Roques, *FEBS Lett.*, **26**, 169 (1972).
17. J. Carbajo, C. Adán, A. Rey, A. Martínez-Arias and A. Bahamonde, *Appl. Catal. B: Environ.*, **102**, 85 (2011).
18. R. B. Bowman, Z. Li, S. J. Roy, T. A. Burt, T. L. Johnson and R. L. Johnson, *Pilot test of a surfactant-modified zeolite permeable barrier for groundwater remediation. Physical and chemical remediation of contaminated aquifers*, Kluwer Academic Publishers, New York (2001).
19. A. Khan, J. E. Szulejko, K. H. Kim, P. Sammadar, S. S. Lee, X. Yang and Y. S. Ok, *Environ. Res.*, **168**, 96 (2019).
20. S. Guggenheim and A. F. K. Groos, *Clays Clay Miner.*, **49**, 433 (2001).
21. P.-H. Chang, Z. Li, W.-T. Jiang and J-S. Jean, *Appl. Clay Sci.*, **46**, 27 (2009).
22. P.-H. Chang, J.-S. Jean, W.-T. Jiang and Z. Li, *Colloids Surf. A*, **339**, 94 (2009).
23. CMS, http://www.clays.org/sourceclays_data.html.
24. U.S. Geological Survey, Mineral commodity summaries 2019: U.S. Geological Survey, 200 p. (2019), https://doi.org/10.3133/70202434.
25. H. H. Eldaroti, S. A. Gadir, M. S. Refat and A. M. A. Adam, *Spectrochim. Acta Part A*, **109**, 259 (2013).

Supporting Information

High capacity ethidium bromide removal by montmorillonites

Lijuan Wang*, **Zhaohui Li*,**,†**, **Xingrong Zhang*****, **Guocheng Lv***, and **Xisen Wang******

*Beijing Key Laboratory of Materials Utilization of Nonmetallic Minerals and Solid Wastes,
National Laboratory of Mineral Materials, School of Materials Science and Technology,
China University of Geosciences, Beijing, 29 Xueyuan Road, Beijing, China 100083
**Department of Geosciences, University of Wisconsin - Parkside, 900 Wood Road, Kenosha, WI 53144, USA
***BGRIMM Technology Group, Beijing 110160, China
****Department of Chemistry, University of Wisconsin - Parkside, 900 Wood Road, Kenosha, WI 53144, USA

(*Received 1 May 2020 • Revised 7 July 2020 • Accepted 11 July 2020*)

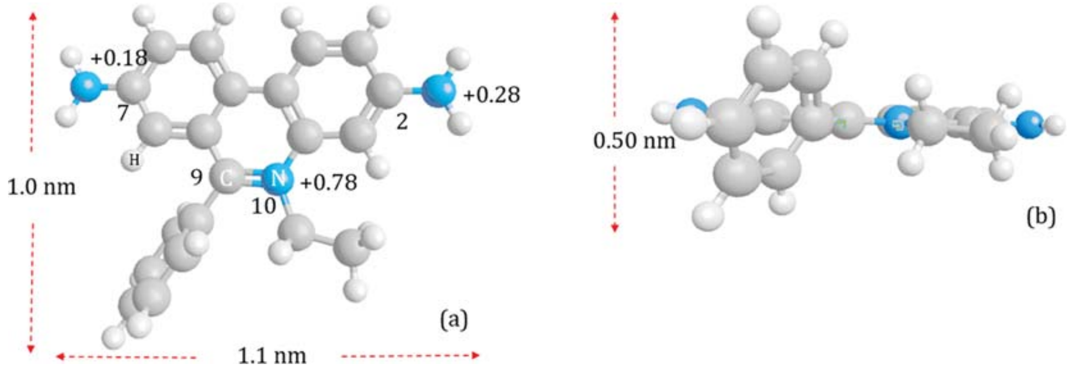

Fig. S1. Molecular structure of EtBr from top (a) side (b) view. The positive values indicated partially positive charge associated with N (blue). The most positively charged N (+0.78) is at location 10.

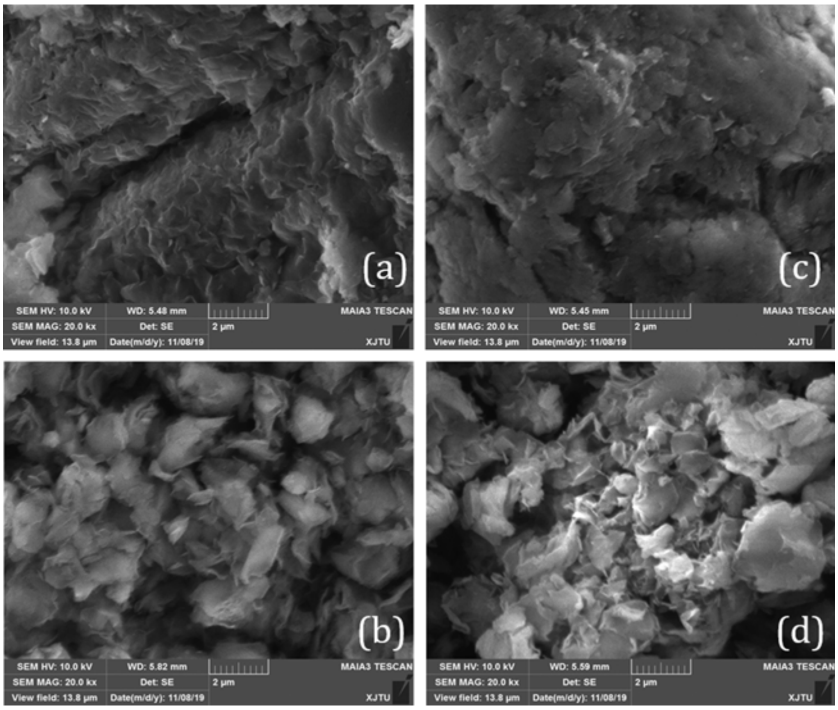

Fig. S2. SEM observation of SAz-2 (a) and SWy-2 (b) after uptake of EtBr and after their regeneration at 500 °C (c), (d).